Density functional theory study of the nematic-isotropic transition in an hybrid cell

I. Rodríguez-Ponce,[1] J. M. Romero-Enrique,[2,3] and L. F. Rull[2]

[1]*Physik Department, Technische Universität München, James-Franck-Strasse, D-85747 Munich, Germany*

[2]*Departamento de Física Atómica, Molecular y Nuclear, Area de Física Teórica, Universidad de Sevilla, Apartado de correos 1065, 41080 Sevilla, Spain*

[3]*Department of Mathematics, Imperial College 180 Queen's Gate, London SW7 2BZ, United Kingdom*

Abstract

We have employed the Density Functional Theory formalism to investigate the nematic-isotropic capillary transitions of a nematogen confined by walls that favor antagonist orientations to the liquid crystal molecules (hybrid cell). We analyse the behavior of the capillary transition as a function of the fluid-substrate interactions and the pore width. In addition to the usual capillary transition between isotropic-like to nematic-like states, we find that this transition can be suppressed when one substrate is wet by the isotropic phase and the other by the nematic phase. Under this condition the system presents interface-like states which allow to continuously transform the nematic-like phase to the isotropic-like phase without undergoing a phase transition. Two different mechanisms for the disappearance of the capillary transition are identified. When the director of the nematic-like state is homogeneously planar-anchored with respect to the substrates, the capillary transition ends up in a critical point. This scenario is analogous to the observed in Ising models when confined in slit pores with opposing surface fields which have critical wetting transitions. When the nematic-like state has a linearly distorted director field, the capillary transition continuously transforms in a transition between two nematic-like states.

I. INTRODUCTION

The effect on confinement on simple fluids has been vastly investigated in the past. Most of studies are related to the effect of the confinement on the vapor-liquid transition, the so-called capillary transition. In the case of symmetric walls, where both walls attract or repel the molecules with the same strength, the capillary transition in large pores is governed by the well-known Kelvin law[1]. In addition, it may appear surface phenomenology that can affect the global phase diagram. Often this surface phenomenology is related to wetting states found in the single wall cases. The latter phenomenon is related to the spreading of drops of vapor (liquid) on the surface in coexistence with the bulk liquid (vapor). The presence of these surface states can be considered in the description of the phase behavior in the confined system. The generalized Kelvin law for small pores (where surface phenomenology is more dominant) takes into account these effects so it is still possible to determine the vapor-liquid transition for small pores[2]. However, the predictions of the generalized Kelvin law reveal that the wetting phenomena does not affect essentially the phase diagram of the confined problem so they are often discarded. An interesting system is the *hybrid* cell (also known as asymmetric cell) where one substrate or wall is repulsive and the other attractive (competing walls). In this case, the wetting properties present in the single wall cases play a crucial role in the determination of the critical point in the confined problem. Here, given a pore width, the coexistence of two phases can only occur for temperatures below T_W, which corresponds to the total wetting temperature of the single wall cases[3,4].

These studies have elucidated which mechanisms are involved in the surface transitions and how the properties of the substrate can determine the phase behavior within the pore. With respect to complex fluids like liquid crystal (LC) there is an increasing interest in the understanding of the surface phenomena due to its crucial role in the advance of the LC technology. For the case of a single wall (semi-infinite problem) and symmetric pores favoring an specific orientation on the molecules, theoretical approaches[5,6,7,8,9,10,11] as well as computer simulations[12,13,14,15,16] reveal that the interaction wall-fluid particle can affect strongly the ordering not only close to the surface but also far from it. Additionally to finite size effects, novel phenomena often appear due to the combined presence of anchoring and orientational wetting transitions. The interplay between both surface phenomena and its dependence on wall properties have been recently studied by us employing a microscopic

Density Functional Theory (DFT) approach for a simple model of liquid crystal[17]. The effect of confinement by symmetric walls on these surface transitions was also studied[18]. Our findings revealed that as in the case of simple fluids, the finite-size effects for not very narrow pores on the phase diagram are not of qualitative significant importance and only the location of the capillary transitions are affected by the confinement. However, recent theoretical[19,20] and simulation results[19] for hard-spherocylinder models show that for very narrow symmetrical pores the NI capillary transition may end up in a critical point.

In a recent paper[21], we extended the study to the case with an hybrid cell where the surfaces favor antagonist orientations. This geometry has in LCs a particular interest due to the possible technological applications. This fact has stimulated an increasing interest by experimentalists and theoreticians[19,22,23]. In particular, different nematic-like states with homogeneous and linearly distorted director fields were found to coexist under confinement. In the present paper, our goal is to complete this study with the investigation of the nematic-isotropic (NI) transition within the hybrid cell. Quintana *et al* investigated a similar problem employing a Landau-type theory[24]. They claimed that the NI transition either appears unaffected and its temperature T_{NI} remains unchanged or the transition disappears. Basically what determined the existence of the transition was the value of fluid-wall interaction strength with respect to the value for the first-order wetting transition for the semi-infinite systems. For strength values below this threshold the transition occurs for all wall separations. In contrast, above the threshold, the transition disappears for large pore widths, where interfacial-like states appear. These states are related to the wetting states by isotropic and nematic phase that each wall present in the semi-infinite geometry, respectively.

In this paper we address the same problem of the behavior of the NI capillary transition and its possible disappearance from a more microscopic point of view by using a DFT approach. Our paper is organized as follows. First we briefly present our liquid crystal model in Section II. In Section III we revisit and complete the study of a substrate which favors either planar or homeotropic anchoring in contact with a nematogen fluid at its isotropic or nematic phase. In particular, the different wetting regimes are found. This phenomenology will be a crucial guide to understand the behavior of the fluid under confinement. Section IV is devoted to the study of the fluid adsorbed in a hybrid cell, paying special attention to the disappearance of the NI capillary transitions and the mechanisms involved in it. Finally

we end up with our conclusions.

II. THE MODEL

The theoretical model is a standard generalized van der Waals theory based on a perturbative expansion, using a hard-sphere (HS) fluid as reference system[7]. Details on the physical basis of the model and how to obtain its solutions numerically can be found elsewhere[25,26]. Our starting point is the grand potential functional per unit system area A, $\Omega[\rho]/A$, whose functional minimum with respect to the one-particle distribution function, $\rho(\mathbf{r},\hat{\mathbf{\Omega}})$, which depends on both molecular positions $\mathbf{r}$ and orientations $\hat{\mathbf{\Omega}}$, gives the equilibrium structure of the interface. This function, $\rho(\mathbf{r},\hat{\mathbf{\Omega}}) \equiv \rho(z) f(z,\hat{\mathbf{\Omega}})$, contains a mass distribution $\rho(z)$ and an angular distribution $f(z,\hat{\mathbf{\Omega}})$. These quantities vary locally with the distance from $z=0$ to $z=H$, where H is the pore width. The expression for $\Omega[\rho]$, in a mean field approximation is,

$$\Omega[\rho] = F_r[\rho] + \frac{1}{2}\int\int\int\int d\mathbf{r}d\mathbf{r}'d\hat{\mathbf{\Omega}}d\hat{\mathbf{\Omega}}'\rho(\mathbf{r},\hat{\mathbf{\Omega}})\rho(\mathbf{r}',\hat{\mathbf{\Omega}}') \times v(\mathbf{r}-\mathbf{r}',\hat{\mathbf{\Omega}},\hat{\mathbf{\Omega}}') - \int\int d\mathbf{r}d\hat{\mathbf{\Omega}}\rho(\mathbf{r},\hat{\mathbf{\Omega}})[\mu - v_W(\mathbf{r},\hat{\mathbf{\Omega}})], \quad (1)$$

where μ is the chemical potential and

$$F_r[\rho] = \int d\mathbf{r} f_{hs}(\rho(\mathbf{r})) + k_B T \int d\mathbf{r}\rho(\mathbf{r})\langle \ln(4\pi f(z,\hat{\mathbf{\Omega}}))\rangle \quad (2)$$

is the reference system free energy. In the above expression $f_{hs}(\rho(\mathbf{r}))$ is the hard-sphere free energy density of a uniform fluid with a density equal to the local density at $\mathbf{r}$ and $\langle \ldots \rangle$ is an angular average. The attractive potential v contains anisotropic (dispersion) forces driving the liquid-crystalline behavior of the model material:

$$v(\mathbf{r},\hat{\mathbf{\Omega}},\hat{\mathbf{\Omega}}') = v_A(r) + v_B(r)P_2(\hat{\mathbf{\Omega}}\cdot\hat{\mathbf{\Omega}}') + v_C(r)\left[P_2(\hat{\mathbf{\Omega}}\cdot\hat{\mathbf{r}}) + P_2(\hat{\mathbf{\Omega}}'\cdot\hat{\mathbf{r}})\right], \quad (3)$$

where $\hat{\mathbf{r}} = \mathbf{r}/r$, and r is the center-of mass distance. The functions $v_A(r)$, $v_B(r)$, $v_C(r)$ are the radial contribution to the potential as a result of considering dispersion-type forces. In this work we choose them to have a simple Yukawa form, i.e. $v_i(r) = -\epsilon_i \exp(-\lambda_i(r-d))/r$ for $r > d$, and $v_i(r) = 0$ otherwise, where d is the diameter of a hard sphere. We note that a positive value of ϵ_C favors the molecule to orientate parallel to the NI interface

and a negative value favors the perpendicular orientation to NI interface. This *anisotropy* in the orientational configuration of the nematic molecules is essential to understand the phenomenology in the problem with the walls.

The walls are modelled via the following potentials:

$$v_W^1(z,\theta) = \begin{cases} +\infty & z < 0 \\ -\epsilon_W^1 e^{-\lambda_W (z-d)} P_2(\cos\theta) & z > 0 \end{cases} \tag{4}$$

where θ is the angle between the molecule axis and the z-axis normal to the substrate. For $\epsilon_W^1 > 0$, this potential favors the molecules to align perpendicularly to the surface (homeotropic anchoring). The potential corresponding to the other substrate is:

$$v_W^2(z,\theta) = \begin{cases} +\infty & z > H \\ \epsilon_W^2 e^{-\lambda_W (-(H-z)-d)} P_2(\cos\theta) & z < H \end{cases} \tag{5}$$

which favors the molecules to align in a plane parallel to the surface for $\epsilon_W^2 > 0$. However, this preferred alignment corresponds to a random planar anchoring, since there is not a preferred direction at the xy orientation plane. The parameters ϵ_W^1 and ϵ_W^2 measure the substrate-fluid interaction strength of each substrate.

In our study, we will assume that the nematic director orientation is embedded in the xz plane. The formalism permits to define the orientation distribution of the molecules referred to a laboratory reference system, described by three order parameters,

$$\eta(z) = \int d\phi \sin\theta d\theta f(z,\hat{\Omega}) P_2(\cos\theta) \tag{6}$$

$$\nu(z) = \int d\phi \sin\theta d\theta f(z,\hat{\Omega}) \sin 2\theta \cos\phi \tag{7}$$

$$\sigma(z) = \int d\phi \sin\theta d\theta f(z,\hat{\Omega}) \sin^2\theta \cos 2\phi \tag{8}$$

The order also can be referred to an intrinsic reference system by three quantities: ψ the *tilt* angle defined like the angle formed by the director with the z axis, U (uniaxial order parameter) the amount of order along the director and B (biaxial order parameter) which measures the amount of order along the perpendicular directions of the director. The nematic ordering is essentially uniaxial ($B = 0$) far from the substrate. The biaxiality induced by the surfaces was already discussed in a previous paper[21].

These intrinsic order parameters can be obtained in terms of the set $\{\eta, \sigma, \nu\}$ by the following expressions,

$$\tan\psi(z) = \frac{\nu(z)}{\eta(z) - \frac{\sigma(z)}{2} + \sqrt{\left[\eta(z) - \frac{\sigma(z)}{2}\right]^2 + \nu(z)^2}} \tag{9}$$

$$U(z) = \frac{\eta(z)}{4} + \frac{3}{8}\sigma(z) + \frac{3}{4}\sqrt{\left[\eta(z) - \frac{\sigma(z)}{2}\right]^2 + \nu(z)^2} \tag{10}$$

$$B(z) = \frac{\eta(z)}{2} + \frac{3}{4}\sigma(z) - \frac{1}{2}\sqrt{\left[\eta(z) - \frac{\sigma(z)}{2}\right]^2 + \nu(z)^2} \tag{11}$$

It is convenient to define the average density and order parameter for the confined system as:

$$\bar{\rho} = \frac{1}{H}\int_0^H \rho(z)dz \tag{12}$$

$$\bar{U} = \frac{1}{H}\int_0^H U(z)dz \tag{13}$$

As we will also make reference to the semi-infinite problems, the adsorption in the order parameter is defined as:

$$\Gamma = \int_0^\infty (U - U_b)dz \tag{14}$$

where U_b is the value of the intrinsic nematic order parameter of the bulk phase.

Numerical values for the potential parameters were taken as $\epsilon_A = 1$ (which sets the temperature scale), $\epsilon_B/\epsilon_A = 0.847$ and $\epsilon_C/\epsilon_A = 0.75$. The range parameters λ_i are set, in units of d (throughout we choose this unit to set the length scale), to $\lambda_i = 2, 4, 1.75$, $i = A, B, C$ respectively, and $\lambda_W = 1$. In our calculations the temperature is fixed at the value $T^* \equiv k_B T/\epsilon_A = 0.57$, that corresponds to a typical situation in which vapor, isotropic and nematic phases can be observed. At this temperature, the isotropic-nematic coexistence occurs for a reduced chemical potential $\beta\mu \equiv \mu/k_B T = -3.918$.

III. THE SEMI-INFINITE CASE.

In order to better understanding the behavior of the fluid inside the pore, we have first considered the semi-infinite cases of the fluid in presence of a single substrate that either favors homeotropic or planar alignment, i.e. the substrate-fluid interaction potentials are

given by Eq. (4) with $\epsilon_W^1 > 0$ or $\epsilon_W^1 < 0$, respectively. We are interested in the wetting behavior, so the system will be at bulk nematic-isotropic coexistence, unless stated otherwise. We have considered both situations in which the bulk fluid is either isotropic or nematic.

First we consider the case of a nematic bulk phase in presence of the substrate. This situation was studied for substrates that favor homeotropic anchoring in Ref. 17. We extend this analysis to substrates which favor planar alignment. For both negative and small positive values of ϵ_W^1 the fluid far from the substrate orientates parallel to the substrate. For the case in which $\epsilon_W^1 < 0$, biaxiality is developed in a microscopic layer close to the substrate, leading to the decay of the orientational order in that area. If the substrate favors a homeotropic alignment, we observe a microscopic isotropic-like layer close to the substrate, corresponding to a partial wetting situation of the substrate-nematic interface by the isotropic phase. As ϵ_W^1 is increased, the isotropic layer close to the substrate becomes macroscopic as the isotropic phase completely wets the nematic-substrate interface at $\epsilon_W^1 = \epsilon_W^{w1}$. Our calculations showed that the wetting transition is continuous. The orientation far from the substrate remains planar in the complete wetting case. By further increasing ϵ_W^1, an anchoring transition occurs for $\epsilon_W^1 = \epsilon_W^d$, as the nematic orientation changes from planar to homeotropic far from the substrate, and the wetting becomes partial again since the isotropic-nematic interface favors a planar anchoring in our model. The anchoring transition is first order and continues in the single nematic phase region. However, the complete wetting with planar orientation state remains metastable up to ϵ_W^m. This fact will be important for the discussion of the confined cases. For the model parameters considered in this paper, $\epsilon_W^{w1}/\epsilon_A = 0.470$, $\epsilon_W^d/\epsilon_A = 0.527$ and $\epsilon_W^m/\epsilon_A = 0.72$.

We turn to the case in which there is an isotropic phase in bulk. For small values of $|\epsilon_W^1|$, the inhomogeneities of the density and order parameter profiles are restricted to a microscopic layer close to the substrate. Although the fluid is isotropic far from the substrate, the anisotropic character of the substrate-fluid potential induces a random planar ordering near the substrate, i.e. the particles orientate parallel to the substrate but without any preferred direction in that orientation plane ($\eta < 0$, $\sigma = \nu = 0$). Such a condition can be seen as an extreme biaxial case, where $B = 2U$, i.e. the highest eigenvalue of the orientational order parameter tensor is twofold degenerate. The layer width remains microscopically finite as the NI coexistence is approached, corresponding to a partial wetting situation. For large enough values of $|\epsilon_W^1|$, we observe complete wetting situations. For negative values of ϵ_W^1 and

at the NI coexistence, there is a sudden change at $\epsilon_W^1 = \epsilon_W^{w2}$ from the previous surface state to a complete wetting state of the isotropic-substrate interface by the nematic phase. This corresponds to a first order wetting transition. For our model parameters, $\epsilon_W^{w2}/\epsilon_A = -0.359$. Due to its first order character, there is a prewetting first-order transition for $\epsilon_W < \epsilon_W^{w2}$ (see Fig. 1). At this transition the particles at the first layer orientates along some direction parallel to the substrate, breaking the rotational symmetry of the state (see insets of Fig. 1 for the order parameter profiles). Consequently, the prewetting transition can be seen as a two-dimensional isotropic to nematic transition at the fluid layer close to the substrate. We will denote I and I^N to the surface states with the random planar and nematic layer close to the wall, respectively. For the I^N state, there is also biaxiality near the substrate, as occurred when there was a nematic fluid in bulk. A similar behavior was found for the Zwanzig model and hard spherocylinder fluids[19], although their "prewetting" transition is continuous (second order for the Zwanzig model and it is expected to be Kosterlitz-Thouless-like for the spherocylinder system). The prewetting surface nematization transition shifts towards lower chemical potentials as ϵ_W is increased, and eventually disappears at a critical point.

For large positive values of ϵ_W^1, i.e. $\epsilon_W^1/\epsilon_A > \epsilon_W^{w3}/\epsilon_A = 0.691$, we also found that the nematic phase completely wets the isotropic-substrate interface. We have checked indirectly this by studying the numerically obtained profiles that minimize our free energy functional. The order parameter profiles that we obtain in our numerical minimization are inhomogeneous along the wetting layer (see Fig. 2). This fact is due to the mismatch of anchoring conditions at the interfaces. We first note that the *intrinsic* order parameters are homogeneous along the wetting layer except close to the interfaces (see inset in Fig. 2). So the origin of the inhomogeneity of the *extrinsic* order parameters is the change of the orientation of the nematic director field along the wetting layer. As previously mentioned, the molecules align parallel to the interface between a nematic and isotropic phase. On the other hand, the molecules anchor homeotropically close to the substrate due to the strong anchoring coupling between the substrate and the fluid. As the nematic layer width diverges, it is possible to fulfill both anchoring conditions by slowly varying the nematic director from homeotropic to planar anchoring. However, any numerical calculation requires minimization in a finite range R for the z coordinate, imposing bulk isotropic conditions for $z > R$. In this situation, the nematic director profile that corresponds to the minimum of the grand-canonical free

energy is expected to be linear, as it is indeed observed by numerical minimization (see inset of Fig. 2). This fact induces a $1/R$ dependence of the apparent equilibrium excess grand-canonical free energy (or surface tension Σ) due to the elastic deformation. Such decay is much slower than the usual exponential correction when elastic deformations are not involved, and we have to consider much larger values of R to obtain reliable values of the true equilibrium free energies. As R increases, the apparent surface tension decreases and it is always larger than the complete wetting state excess free energy, that it is the sum of the surface tension Σ_{wN} corresponding to the interface between substrate and a nematic phase oriented homeotropically far away, and the surface tension Σ_{NI} between corresponding to the nematic-isotropic interface where the nematic phase is planar-anchored with respect to the interface. The latter surface tension is independent of the fluid-substrate interactions, and its value is $\beta\Sigma_{NI}d^2 \approx 0.0259$ for the NI coexistence at $T^* = 0.57$.

Fig. 3 summarizes the results of this Section. We represent the cosine of the contact angle θ of a droplet of isotropic phase in coexistence with bulk the nematic phase on a planar substrate as a function of ϵ_W. The Young equation states that:

$$\cos\theta = \frac{\Sigma_{wN} - \Sigma_{wI}}{\Sigma_{NI}} \tag{15}$$

where Σ_{wN}, Σ_{wI} and Σ_{NI} are the surface tensions corresponding to the substrate-nematic, substrate-isotropic and nematic-isotropic interfaces, respectively. For $\epsilon_W < \epsilon_W^d$ (including negative values), the nematic director is parallel to the substrate far from the substrate. Otherwise, the nematic director is homeotropically anchored. The complete wetting region corresponds to $\cos\theta = 1$. The curve meets the $\cos\theta = 1$ line at $\epsilon_W = \epsilon_W^{w1}$ with no change in slope. This fact is a signature of the second-order character of the wetting transition. On the contrary, the curve departs from the $\cos\theta = 1$ line at $\epsilon_W = \epsilon_W^d$ with non-zero slope, indicating the first-order character of the dewetting transition.

Fig. 3 also gives information about the wetting properties when there is an isotropic phase in bulk. By reversing the roles of the nematic and isotropic phases in Eq. (15), it is straightforward to see that the contact angle θ' of a nematic droplet on a planar substrate is related to θ via $\theta' = \pi - \theta$. Consequently, when $\cos\theta = -1$ we observe complete wetting by nematic phase of the isotropic-substrate interface. This fact is clear for $\epsilon_W < \epsilon_W^{w2} < 0$. However, for $\epsilon > \epsilon_W^{w3}$ the apparent values of $\cos\theta$ are less than -1. As previously discussed, this is a finite-size effect of our numerical calculations and the predicted value is $\cos\theta = -1$.

Nevertheless, since the nematic layer remains finite as $\epsilon_W \to \epsilon_W^{w3}$ from below, the localization of the wetting transition is quite accurate. For both wetting transitions at ϵ_W^{w2} and ϵ_W^{w3} there is a change of slope of the $\cos\theta$ curve, that it is in agreement with their first-order character.

IV. THE CONFINED CASE.

We turn to the case of the fluid confined in a hybrid slit pore, where each substrate favors an antagonist anchoring, i.e. homeotropic and planar, respectively. Under confinement, it is well known that the bulk transitions have lower-dimensional counterparts that are known as capillary transitions. The thermodynamic conditions (temperature, pressure, chemical potential) for such transitions are usually shifted with respect to the bulk coexistence values. Before considering our DFT results, we consider the predictions of the Kelvin equation, which gives the leading order for the shift on chemical potential $\Delta\mu = \mu_{NI}^c - \mu_{NI}^b$ of the capillary nematic-isotropic transition μ_{NI}^c with respect to the bulk value μ_{NI}^b at large pore widths H. Thermodynamic considerations[2,20,27] show that the chemical potential shift $\Delta\mu$ of a capillary transition with respect to the bulk one between the α and β phases at a given temperature obeys asymptotically:

$$\Delta\mu \approx \frac{\Sigma_{\alpha\beta}(\cos\theta_1 + \cos\theta_2)}{(\rho_\beta - \rho_\alpha)H} \tag{16}$$

In this expression, $\Sigma_{\alpha\beta}$ is the surface tension for an $\alpha - \beta$ interface, and ρ_α and ρ_β are the bulk densities of the α and β phases, respectively. Finally, θ_1 and θ_2 are the contact angles corresponding to the droplets of α phase that nucleate on each substrate when the fluid is in bulk in the β phase, respectively. In our case, we can identify α as the isotropic phase and β as the nematic phase. It is implicitely assumed in Eq. (16) that there is a partial wetting situation for both substrates in semi-infinite geometries. However, if either there is complete wetting only at one substrate or in both but by the same phase ($\theta_1 = \theta_2 = 0$ or π), the effective pore width in Eq. (16) is reduced to $H - \kappa l$, where κ is a constant that depends on the range of the wall-fluid interactions and l is the sum of the widths of the adsorbed wetting layers. Nevertheless, this modification does not change qualitatively the results. Its only effect is to observe the behavior predicted by the Kelvin equation at larger values of the pore width H than for a partial wetting situation.

A different situation arises when both substrates are completely wet by *different* phases at

coexistence, i.e. $\cos\theta_1 \cos\theta_2 = -1$. Studies for symmetrically opposing surface fields Ising systems[3,4] and Landau-de Gennes models of liquid crystals[24] show that in this situation there is *no* capillary transition. Instead, an interface-like state appears, where half the pore is filled with an α-like layer, and the rest by β-like phase. The position of the interface between both layers is controlled by the deviation of chemical potential with respect to the coexistence value, being possible to go from an α-like capillary pure phase to a β-like one without undergoing any phase transition. The phase transition is only recovered in the bulk limit $H = \infty$. When the opposing surface fields are not symmetrical (at least for near-symmetrical), it is expected to observe a similar behavior[3].

This analysis allows us to envisage different scenarios for the confined case and large H. For simplicity, we will only consider the case $\epsilon_W^1 = \epsilon_W^2 \equiv \epsilon_W$ in Eqs. (4) and (5). We must note that this choice *does not* correspond to the symmetrical opposing fields, since the effect of each substrate is qualitatively different. For large H and $\epsilon_W/\epsilon_A < 0.48$ and $\epsilon_W/\epsilon_A > 0.53$ we expect to have a nematic-isotropic capillary transition. The transition point will shifted towards lower or higher chemical potentials than the corresponding to the bulk transition if $\cos\theta_1 + \cos\theta_2$ is negative or positive, respectively. This state-dependent capillary transition shift, which does not occur for simple fluids, has been observed in our model under confinement between symmetrical substrates that favor homeotropic anchoring[18], and also in confined spherocylinder model with the Onsager approximation for a symmetrical slit pore[20]. On the other hand, if $0.48 < \epsilon_W/\epsilon_A < 0.53$, no capillary transition is expected to be obtained for *any* pore width.

We present now our DFT calculations. For the sake of clarity, we separate the results obtained for $\epsilon_W < \epsilon_W^{w1}$ and $\epsilon_W > \epsilon_W^{d}$.

A. The case $\epsilon_W < \epsilon_W^{w1}$

We performed our first DFT calculations for $\epsilon_W/\epsilon_A = 0.30$, which correspond to partial wetting situation in the semi-infinite geometry for both substrates. Fig. 4 shows the behavior of the averaged intrinsic order parameter $\bar{U}$ as the chemical potential is varied. We see that there is a transition from an isotropic-like state (lower branch) to a nematic-like state (upper branch). The order of the transition is first-order, and it is found as the coincidence point of the grand-canonical free energies of the nematic-like and isotropic-like states. We have

shown also the metastable continuations of each branch: nematic-like states on the left of the capillary NI transition and isotropic-like states on the right of the transition. Examination of the order parameter profiles show that the director field in the nematic-like state is oriented parallel throughout the pore to the substrate with an intrinsic order parameter similar to the bulk value, except in thin layers around the substrates, where the density and order parameter profiles are similar to the ones corresponding to the semi-infinite cases. In particular a very thin layer close to the $z = 0$ substrate is homeotropically anchored. This state corresponds to the S state in Ref. 21 and we will denote it by N^S. On the other hand, the isotropic-like state (which we will denote as I) develops microscopic homeotropically and random-planar layers close to the $z = 0$ and $z = H$ substrates, respectively, and the orientational ordering decays to zero in the middle region of the pore. We have also compared our DFT calculations with the Kelvin law prediction Eq. (16) (see inset in Fig. 4). Although the transition value departs from this prediction for small pore widths, for $H/d > 20$ the agreement between our numerical estimations and the Kelvin predicted value is quite reasonable. Note that the capillary NI transition is shifted to larger chemical potentials than the bulk NI transition value. However, as ϵ_W increases, this trend is reversed (the Kelvin law predicts the turning point to occur at $\epsilon_W/\epsilon_A = 0.329$).

As ϵ_W exceeds ϵ_W^{w2}, wetting in the $z = H$ wall begins to affect the pore adsorption. For small values of H a single transition between an isotropic-like I state to a nematic-like state occurs as for $\epsilon_W < \epsilon_W^{w2}$. However, as H increases the order of the "nematic-like" state decreases and the chemical potential for which this transition occurs converges to the $I - I^N$ transition value for the $z = H$ wall. The order-parameter profiles make clear that the "nematic-like" state corresponds to the formation of a nematic layer close to the $z = H$ substrate followed by an isotropic ordering along the pore. By analogy with the semi-infinite situation, we call I^N to the confined state after this transition, which we can see as a reminiscence of the $I - I^N$ transition in the semi-infinite phenomenology.

As H increases, in addition to the $I - I^N$ transition, a new phase transition between the I^N to a proper nematic-like state N^S (i.e. planar-anchored along the pore) is observed. This transition can be regarded as the true capillary NI transition. Fig. 5 shows our DFT calculations for $H = 20d$ and different values of ϵ_W. It becomes clear that the difference between the I^N and the N^S states at the transition decreases as ϵ_W increases, and eventually the NI capillary transition disappears in a critical point (see inset of Fig. 5). The value of

ϵ_W at which the NI capillary transition disappears is *lower* than ϵ_W^{w1}, i.e. the confinement *distabilizes* the two-phase region with respect to the one-phase region. We have also studied the effect of the pore width in the NI capillary transition. We set $\epsilon_W/\epsilon_A = 0.465$, slightly below ϵ_W^{w1}. Fig. 6 shows that the capillary NI transition does not exist for the smallest values of H and reappears for $H > 50d$.

The disappearance of the NI capillar transition shown by our model is not related to the critical points observed for *small* values of H in other models[19,20]. Actually, those cases correspond to symmetrical slit-pores and consequently their phenomenology is not related to wetting properties of the substrates. In our model the NI capillary transition occurs at least for $H > 20d$ when the substrates at $z = 0$ and $z = H$ are the same[18]. However we cannot rule out the possibility of critical points for very small H, but we will not consider them since the predictions of our model are not reliable in that regime.

Our DFT results about the existence of the NI capillary transition show the opposite trend to the one predicted by a Landau-de Gennes model in Ref. 24, which predicted that the confinement *stabilized* the two-phase region with respect to the one-phase region. Moreover for large values of H the boundary for the non-existence region of the capillary transition was a triple point rather than a critical point. Actually the scenario shown by our DFT calculations is consistent with the phenomenology that presents a confined Ising model with opposing surface fields when the wetting transition is critical[3]. This analogy can be explained heuristically. For large H and ϵ_W close to ϵ_W^{w1}, the typical configuration close to bulk coexistence corresponds to an interfacial state formed by an isotropic layer around the $z = 0$ and a nematic layer around the $z = H$ wall. In first approximation the NI interface position is given by the minimum binding potential which is the superposition of the contributions from the two semi-infinite systems[3]. As there is a complete wetting situation at the $z = H$ substrate, we can consider its binding potential as a exponentially decreasing function of the interfacial position with respect to the $z = H$ wall $c\exp[-(H - l)/\xi_b']$, where $c > 0$ and ξ_b' is the nematic phase correlation length at bulk NI coexistence. Note that the local minimum corresponding to the bounded state, if any, plays no role in our argument as soon as we are far enough from the first-order wetting transition corresponding to the semi-infinite case with the $z = H$ wall. On the other hand, the binding potential corresponding to the $z = 0$ substrate takes the usual form $-a\exp(-l/\xi_b) + b\exp(-2l/\xi_b)$, where $a \propto \epsilon_W^{w1} - \epsilon_W > 0$, $b > 0$ and ξ_b is the isotropic phase correlation length at bulk

NI coexistence. So, the complete binding potential for the NI interfase, up to irrelevant constants, is:

$$W(l) = h(H-l) - ae^{-\frac{l}{\xi_b}} + be^{-\frac{2l}{\xi_b}} + ce^{-\frac{H-l}{\xi_b'}} \tag{17}$$

where $h \propto \Delta\mu$. A critical point must verify:

$$h = \frac{a}{\xi_b}e^{-\frac{l}{\xi_b}} - \frac{2b}{\xi_b}e^{-\frac{2l}{\xi_b}} + \frac{c}{\xi_b'}e^{-\frac{H-l}{\xi_b'}} \tag{18}$$

$$0 = -\frac{a}{\xi_b^2}e^{-\frac{l}{\xi_b}} + \frac{4b}{\xi_b^2}e^{-\frac{2l}{\xi_b}} + \frac{c}{(\xi_b')^2}e^{-\frac{H-l}{\xi_b'}} \tag{19}$$

Instead of solving simultaneously Eqs. (18) and (19), we will study the spinodal line, which is the solution of Eq. (19). We consider solutions of the form $l \equiv \chi H + \Delta l$, where $0 < \chi < 1$ and $\Delta l \sim \xi_b, \xi_b'$. Substituting this ansatz in Eq. (19), we obtain

$$\begin{aligned} 0 = & -\left(ae^{-\frac{\chi H}{\xi_b}}\right)e^{-\frac{\Delta l}{\xi_b}} + \left(4be^{-\frac{2\chi H}{\xi_b}}\right)e^{-\frac{2\Delta l}{\xi_b}} \\ & + \left(c\frac{\xi_b^2}{(\xi_b')^2}e^{-\frac{(1-\chi)H}{\xi_b'}}\right)e^{\frac{\Delta l}{\xi_b'}} \end{aligned} \tag{20}$$

In order to have two solutions for the Eq. (20), we need all the factors in brackets in Eq. (20) to be of the same order. Consequently we obtain that $\chi = \xi_b/(2\xi_b' + \xi_b)$ and $a = a' \exp[-H/(2\xi_b' + \xi_b)]$, where $a' \sim b \sim c$. The value of a' for which the critical point occurs corresponds to the case where the rescaled equation:

$$0 = -a'e^{-\frac{\Delta l}{\xi_b}} + 4be^{-\frac{2\Delta l}{\xi_b}} + c\frac{\xi_b^2}{(\xi_b')^2}e^{\frac{\Delta l}{\xi_b}} \tag{21}$$

has an unique real solution. For simplicity, we assume that $\xi_b = \xi_b'$, but similar results are found when both correlation lengths are different. We refrain to give explicit solutions and we just mention that indeed $a'/c \sim 1$ and the value of Δl at the critical point is $\Delta l_c \sim \xi_b$ for reasonable values of b and c. Consequently, the interfacial position at the critical point $l_c \sim H/3$ and the NI capillary transition shift $\epsilon_W^{w1} - \epsilon_W \sim \exp(-H/3\xi_b)$ and from Eq. (18) $\Delta\mu \sim \exp(-2H/3\xi_b)$.

A numerical comparison of these predictions with our DFT calculations, although it would be very interesting, is extremely difficult due to the limitations of our numerical procedure and it will not be carried out in this work. However, at least qualitatively these predictions have been confirmed by the DFT calculations even for not so large values of H.

B. The case $\epsilon_W > \epsilon_W^d$

Now we turn to study the confined system for $\epsilon_W > \epsilon_W^d$. We first considered the case $\epsilon_W/\epsilon_A = 0.70$ and $H = 20d$. Different confined states are obtained as the chemical potential increases (see Fig. 7). The first cases Figs. 7(a) and 7(b) clearly correspond to a vapor-like and isotropic-like states, and we will denote them as V and I, respectively. There is in both cases a homeotropically-anchored nematic layer close to the substrate at $z = 0$ and a random planar layer close to the substrate at $z = H$. As the chemical potential increases, the random planar layer at $z = H$ undergoes a transition to a planar biaxial state. Again this first-order transition is a reminiscence of the $I - I^N$ surface transition corresponding to the substrate at $z = H$, and we will denote both confined states I and I^N by analogy with the semi-infinite phenomenology. As the chemical potential is further increased, the nematic layer increases and a state in which an isotropic and a nematic layer coexist is obtained (Fig. 7(c)). There is no phase transition between the isotropic-like I^N and the nematic-like N^S states, but a smooth transformation similar to the expected one when both substrates are completely wet by different bulk phases at coexistence. Finally, there is a transition to a new nematic-like state (the *L state* in Ref. 21, that we will denote as N^L), characterized by an almost linear distorsion from homeotropic to planar configuration on the tilt angle through the pore, although the *intrinsic* order parameter takes essentially the bulk value except close to the substrates (see Fig. 7(d)). This transition between the N^L and N^S state is first order and converges to the anchoring transition that is observed in the semi-infinite case with a substrate that favors a homeotropic anchoring as $H \to \infty$[17]. A more detailed discussion about this transition can be found in Ref. 21.

For larger values of H, the capillary NI transition appears as a transition between an I^N state and a N^L state for chemical potentials smaller than the bulk NI transition value. As ϵ_W approaches ϵ_W^d, the range of values of H for which capillary transition does not exist is wider. For $\epsilon_W/\epsilon_A = 0.53$ (close to the dewetting transition point) the capillary NI transition does not appear until $H/d > 150$. Fig. 8 shows the continuous change of the nematic layer as the chemical potential increases for $H = 20d$, which is analogous to the behavior observed for $\epsilon_W/\epsilon_A = 0.70$. Fig. 9 shows how the curves of the averaged intrinsic order parameter as a function of the chemical potential change for increasing pore widths. For the narrowest pore ($H = 10d$), a single transition is observed between an isotropic state to an state with

some nematic ordering. However, as H is increased, it becomes clear that this transition is again a reminiscence of the $I - I^N$ transition in the semi-infinite case. The localization of this transition depends weakly on the pore width H. For $H > 13d$, the $N^L - N^S$ transition appears at chemical potentials larger than the bulk NI coexistence value. This transition does not appear for $H = 10d$, which is a clear indication of the existence of a critical point for the $N^L - N^S$ transition at small values of H. As H increases, the chemical potential value for $N^L - N^S$ transition shifts to lower values. Finally, we observe that the $\bar{U}$ curve becomes increasingly steep at the bulk NI transition as $H \to \infty$. This fact is a consequence of the formation of interfacial-like states (as Fig. 7(c)) in the proximities of the bulk NI coexistence chemical potential.

The non-existence of a capillary NI transition in the situation described above is unexpected. First, the finite-width effects are much more pronounced for $\epsilon_W > \epsilon_W^d$ than below ϵ_W^{w1}. As a consequence, we observe significant departures from the bulk behavior for wider pores and in a larger range of ϵ_W than when we approach the complete wetting situation from below (i.e. $\epsilon_W < \epsilon_W^{w1}$). This fact suggests the emergence of a new length scale in the system. On the other hand, as the dewetting transition is first order, we could naively expect that under confinement and large enough H the capillary transition disappearance point is shifted to *lower* values of ϵ_W[4,24] (recall that the role of ϵ_W or the temperature is reversed in the dewetting transition with respect to the wetting transition). To understand this situation we recall that the confinement in a hybrid cell distabilizes the N^L with respect to the N^S. A simple phenomenological argument can be used to explain this fact[21]. For large enough values of H, the excess free-energy per surface area of a N^S state is given by the sum of the surface free energies between each substrate and a nematic fluid which is planar-anchored with respect to them. The finite-width corrections are expected to decay exponentially. On the other hand, the large H behavior free energy of the N^L state is the sum of the surface tensions of the interface between the $z = 0$ substrate and a homeotropically-anchored nematic fluid and the corresponding between the planar-anchored nematic fluid and the $z = H$ substrate. For this state the finite-width correction is dominated by the elastic deformations contribution and decays as $K_3\pi^2/8H$ as $H \to \infty$, where K_3 is a Frank-Oseen elastic constant[21]. So, for a given temperature, the $N^S - N^L$ transition is always shifted towards higher chemical potentials than the anchoring transition, and the convergence to it for large values of H is quite slow. Although this argument implicitely assumes that the

inhomogeneities are restricted to microscopic regions around each substrate, it is also valid if we allow the N^S state to develop an isotropic layer close to the $z = 0$ substrate (as occurs close to the bulk NI coexistence). Consequently, for $\epsilon_W^d < \epsilon_W < \epsilon_W^m$ and moderate values of H, the most stable nematic-like state close to the bulk NI coexistence is N^S, and therefore there is no capillary transition. As H increases, the N^L state becomes more stable than the N^S state near the NI bulk transition, and eventually the capillary transition between a I^N state and a N^L occurs.

An interesting feature of the NI capillary transition in this regime is that it is linked to the *purely surface transition* $N^S - N^L$. As explained before, for small values of H there is no NI capillary transition but if H is not too small there is a $N^S - N^L$ transition. As H increases, the chemical potential corresponding to the $N^S - N^L$ transition shifts to smaller values, and eventually crosses the value corresponding to the bulk NI transition (see Fig. 10). When this happens, the transition is between a isotropic-like I^N state to the nematic-like N^L state: the capillary NI transition is recovered. Finally, the Kelvin relationship Eq. (16) predicts that the capillary transition value of $\beta\mu$ approaches the bulk NI value from *below*. The DFT results for large H support this prediction. So, at fixed temperature and chemical potential, and changing H, reentrance of the isotropic-like state is observed (see Fig. 10).

V. CONCLUSIONS

In this paper we have reported a DFT study of the NI capillary transition under confinement in a slit-pore where each substrate favors a different anchoring condition. We found that there is an interplay between the phenomenology found in the semi-infinite problems with the phenomenology which appeared in the confined problem. We have focussed in the non-existence of the NI capillary transition as a result of both substrates to be wet by different phases. If we approach this region from below, we observe a distabilization of the two-phase region with respect to the one-phase region. Moreover, the capillary NI transition finishes in a critical point. These findings are different from the ones reported by Quintana *et al*[24] and this discrepancy can be traced to the different order of the wetting transition. When we approach the non-existence range for the NI capillary transition from above, a different mechanism is involved in the finite-size effects of the capillary NI transition. Al-

though the wetting transition which drives the disappearance of the capillary transition is first-order, the two-phase region is still distabilized with respect to the one-phase region. The explanation for this is the existence of two nematic-like locally stable phases with a relative stability dependent on the pore width. One of them corresponds to a complete wetting situation, so links with the isotropic-like states without undergoing a phase transition. So, as H increases, the phase transition between two nematic-like states transforms continuously to the NI capillary transition. As a consequence, a reentrant behavior for the isotropic-like state is observed by varying the pore width and keeping the temperature and chemical potential constant.

Although we have restricted our study to an isotherm case, we anticipate that we would find a similar behavior if the temperature is changed instead of the value of ϵ_W. On the other hand, the condition $\epsilon_W^1 = \epsilon_W^2$ is not so restrictive as soon as the wetting transition of the $z = H$ wall precedes the complete wetting at the $z = 0$ wall. If such a condition is not fulfilled, our conclusions may change.

Acknowledgments

I.R.P. would like to thank Prof. F. Schwabl for his help in the development of this work and Prof. J. O. Indekeu for useful discussions. J. M. R.-E. also thanks Prof. A. O. Parry for his interest in this work. I.R.P note that this work has been performed under the auspices of the Sonderforschungsbereich (SFB) 563. Financial support by the Deutsche Forschungsgemainschaft (DPG) is gratefully acknowledged. J.M. R.-E. and L.F.R acknowledge finantial support by Grant No. BQU2001-3615-C02-02 from MEC (Spain). Finally, J. M. R.-E. also acknowledges partial financial support from Secretaría de Estado de Educación y Universidades (Spain), co-financed by the European Social Fund, and from the European Commission under Contract MEIF-CT-2003-501042.

---

[1] W. T. Thomson (Lord Kelvin), Phil. Mag. **42**, 448 (1871).

[2] R. Evans, U. Marini Bettolo Marconi, and P. Tarazona, J. Chem. Phys. **84**, 2376 (1986).

[3] A. O. Parry and R. Evans, Phys. Rev. Lett. **64**, 439 (1990); Physica A **181**, 250 (1992).

[4] M. R. Swift, A. L. Owczarek, J. O. Indekeu, Europhys. Lett. **14**, 475 (1991).

[5] J. G. Fonseca and Y. Galerne, Phys. Rev. E **61**, 1550 (2000).

[6] K. Kocevar, I. Musevic, Phys. Rev. E **65**, 021703 (2002).

[7] M. M. Telo da Gama, Molec. Phys. **52**, 611 (1984).

[8] P. I. Teixeira, Phys. Rev. E **55**, 2876 (1997).

[9] A. K. Sen and D. E. Sullivan, Phys. Rev. A **35**, 1391 (1987).

[10] A. Poniewierski and A. Samborski, Liq. Cryst. **27**, 1285 (2000).

[11] R. Seidin, R. M. Hornreich and D. W. Allender, Phys. Rev. E **55**, 4302 (1997).

[12] C. Chiccoli, Y. Lansac, P. Pasini, J. Stelzer and C. Zannoni, Molec. Crys. Liq. Crys. **372**, 157 (2002).

[13] V. Palermo, F. Biscarni and C. Zanoni, Phys. Rev. E **57**, R2519 (1998).

[14] Michael. P. Allen, Molec. Phys. **96**, 1391 (1999).

[15] G. D. Wall and D. J. Cleaver, Phys. Rev. E **56**, 4306 (1997).

[16] N. Priezjev and R. A. Pelcovits, Phys. Rev. E **62**, 6734 (2000).

[17] I. Rodríguez-Ponce, J. M. Romero-Enrique, E. Velasco, L. Mederos and L. F. Rull, Phys. Rev. Lett. **82**, 2697 (1999).

[18] I. Rodríguez-Ponce, J. M. Romero-Enrique, E. Velasco, L. Mederos and L. F. Rull, J. Phys.: Condens. Matter **12**, A363 (2000).

[19] R. van Roij, M. Dijkstra and R. Evans, Europhys. Lett., **49**, 350 (2000).

[20] D. de las Heras, E. Velasco and L. Mederos, J. Chem. Phys. **120**, 4949 (2004).

[21] I. Rodríguez-Ponce, J. M. Romero-Enrique and L. F. Rull, Phys. Rev. E **64**, 051704 (2001).

[22] M. M. Mittenbrood, T. Rasing, S. Stallinga and I. Muševič, Phys. Rev. Lett. **80**, 1232 (1998).

[23] A. Sarlah and S. Žumer, Phys. Rev. E, **60**, 1821 (1999).

[24] J. Quintana and A. Robledo, Physica A **248**, 28 (1998).

[25] F. N. Braun, T. J. Sluckin, E. Velasco and L. Mederos, Phys. Rev. E **53**, 706 (1996). An alternative numerical approach is that used in E. Martín del Río, M. M. Telo da Gama, E. de Miguel and L. Rull, Phys. Rev. E **52**, 5028 (1995).

[26] Y. Martínez, E. Velasco, A. M. Somoza, L. Mederos and T. J. Sluckin, J. Chem. Phys. **108**, 2583 (1998).

[27] A. Poniewierski and T. J. Sluckin, Liq. Cryst. **2**, 281 (1987).

FIG. 1: The adsorption Γ plotted vs. the chemical potential for a semi-infinite geometry where the fluid is isotropic in bulk and the substrate favors homeotropic anchoring. The dashed line corresponds to $\epsilon_W/\epsilon_A = 0.3$ and the continuous line to $\epsilon_W/\epsilon_A = 0.66$. The $I - I^N$ transition for the latter case is represented by the dotted line. The insets represent the reduced density $\rho^* \equiv \rho d^3$ and extrinsic order parameter profiles η, σ and ν for different chemical potentials and $\epsilon_W/\epsilon_A = 0.66$.

FIG. 2: Plot of the reduced density ρd^3 and extrinsic order parameter profiles η, σ and ν for $\epsilon_W/\epsilon_A = 0.70$ and $\beta\mu = -3.918$, obtained by numerical minimization for $R = 435d$. Inset: the intrinsic order parameters U and ψ corresponding to the same state. The intrinsic order parameter B is zero except close to $z = R$ (not shown for clarity).

FIG. 3: Plot of the cosine of the contact angle θ of an isotropic phase droplet on the substrate-nematic interface as a function of the fluid-substrate interaction strength ϵ_W (thick continuous line). The filled circles correspond to the numerical estimates for $\epsilon_W > \epsilon_W^{w3}$ (see text for explanation).

FIG. 4: Plot of the averaged intrinsic order parameter throughout the pore $\bar{U}$ as a function of the reduced chemical potential $\beta\mu$ for $\epsilon_W/\epsilon_A = 0.3$ and $H/d = 10$ (continuous line) and $H/d = 20$ (dashed line). The dotted lines show the location of the capillary NI transition. Inset: the diamonds represent our DFT values of the chemical potential for $\epsilon_W/\epsilon_A = 0.3$ at the capillary NI transition for $H/d = 10$, 20 and 35, and the continuous line is the Kelvin law prediction, Eq. (16).

FIG. 5: Plot of the averaged intrinsic order parameter throughout the pore $\bar{U}$ as a function of the reduced chemical potential $\beta\mu$ for $H/d = 20$ and $\epsilon_W/\epsilon_A = 0.35$ (dashed line), $\epsilon_W/\epsilon_A = 0.41$ (continuous line) and $\epsilon_W/\epsilon_A = 0.45$ (dot-dashed line). The dotted lines show the location of the $I - I^N$ transition (left) and capillary NI transitions (right). Inset: The symbols are the coexistence values of $\bar{U}$ at the $I - I^N$ and capillary NI transitions for different values of ϵ_W. The continuous lines are to guide the eye.

FIG. 6: Plot of the averaged intrinsic order parameter throughout the pore $\bar{U}$ as a function of the reduced chemical potential $\beta\mu$ for $\epsilon_W/\epsilon_A = 0.465$ and $H/d = 10$, 20, 40, 50 and 60.

FIG. 7: Plot of the density ($\rho^* \equiv \rho d^3$) and intrinsic uniaxial order parameter (U) for the fluid confined in a pore of width $H = 20d$ and $\epsilon_W/\epsilon_A = 0.70$ and chemical potentials: (a) $\beta\mu = -4.7$, (b) $\beta\mu = -4.45$, (c) $\beta\mu = -3.95$ and $\beta\mu = -3.7$.

FIG. 8: Density ($\rho^* \equiv \rho d^3$) and intrinsic uniaxial order parameter profiles (U) for $H = 20d$ and $\epsilon_W/\epsilon_A = 0.53$. The chemical potentials run from $\beta\mu = -4.03$ to $\beta\mu = -3.64$ with a step of $\Delta(\beta\mu) = 0.01$.

FIG. 9: Plot of the averaged intrinsic order parameter $\bar{U}$ throughout the pore vs the reduced chemical potential $\beta\mu$ for $\epsilon_W/\epsilon_A = 0.53$ and $H/d = 10$, 13, 20, 30, 40 and 80. The discontinuities of $\bar{U}(\beta\mu)$ correspond to the $I - I^N$ (left) and $N^S - N^L$ (right) transitions.

FIG. 10: Plot of the reduced chemical potential $\beta\mu$ corresponding to the $N^S - N^L$ transition (or the NI capillary transition, see text for explanation) as a function of the reduced inverse pore width d/H for values of $\epsilon_W/\epsilon_A = 0.49$ (circles), 0.53 (diamonds), 0.60 (triangles up) and 0.66 (triangles down). The continuous lines are only to guide the eye.

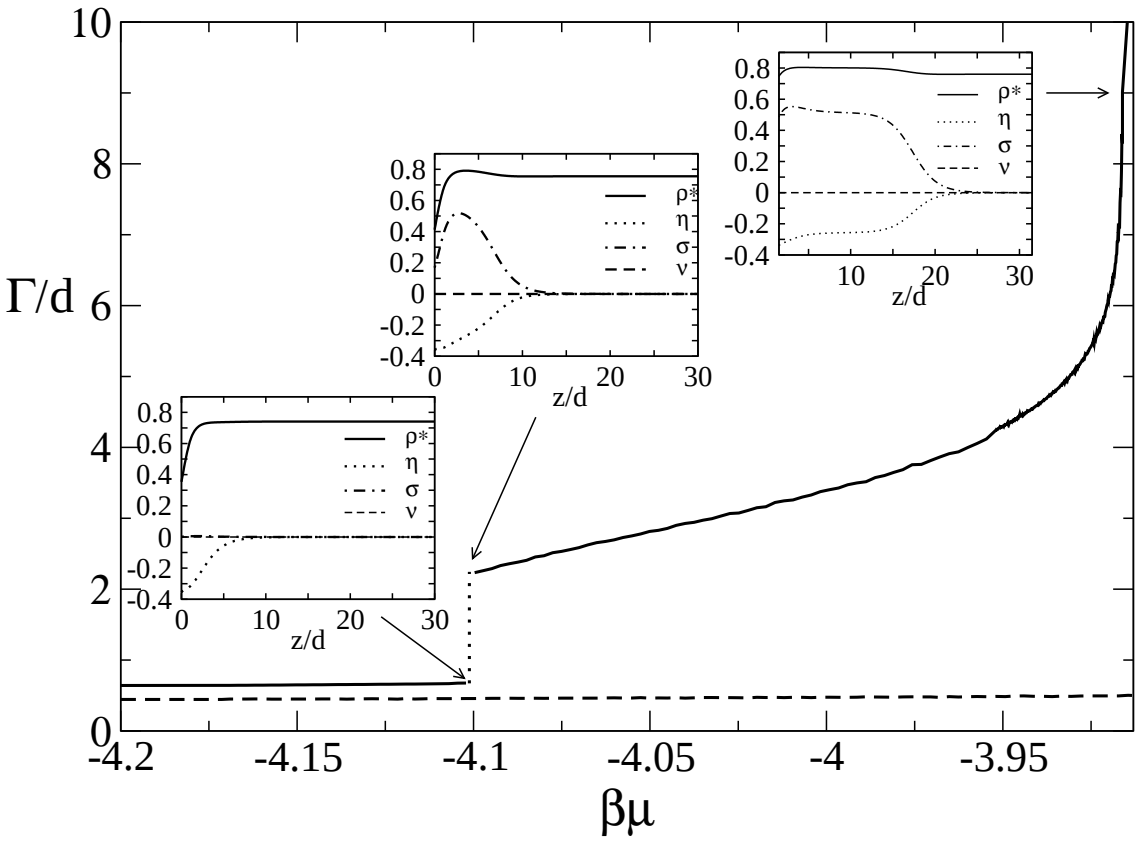

I. RODRIGUEZ-PONCE *et al*, FIGURE 1

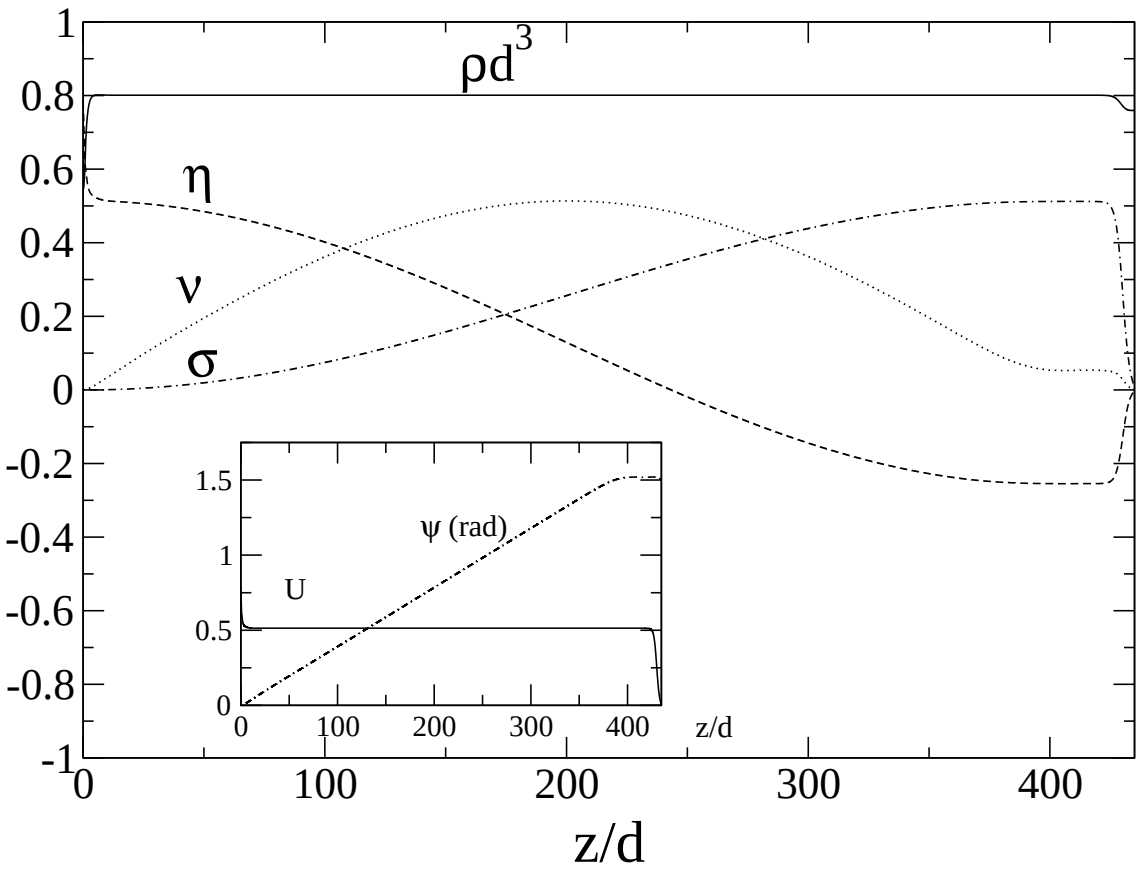

I. RODRIGUEZ-PONCE *et al*, FIGURE 2

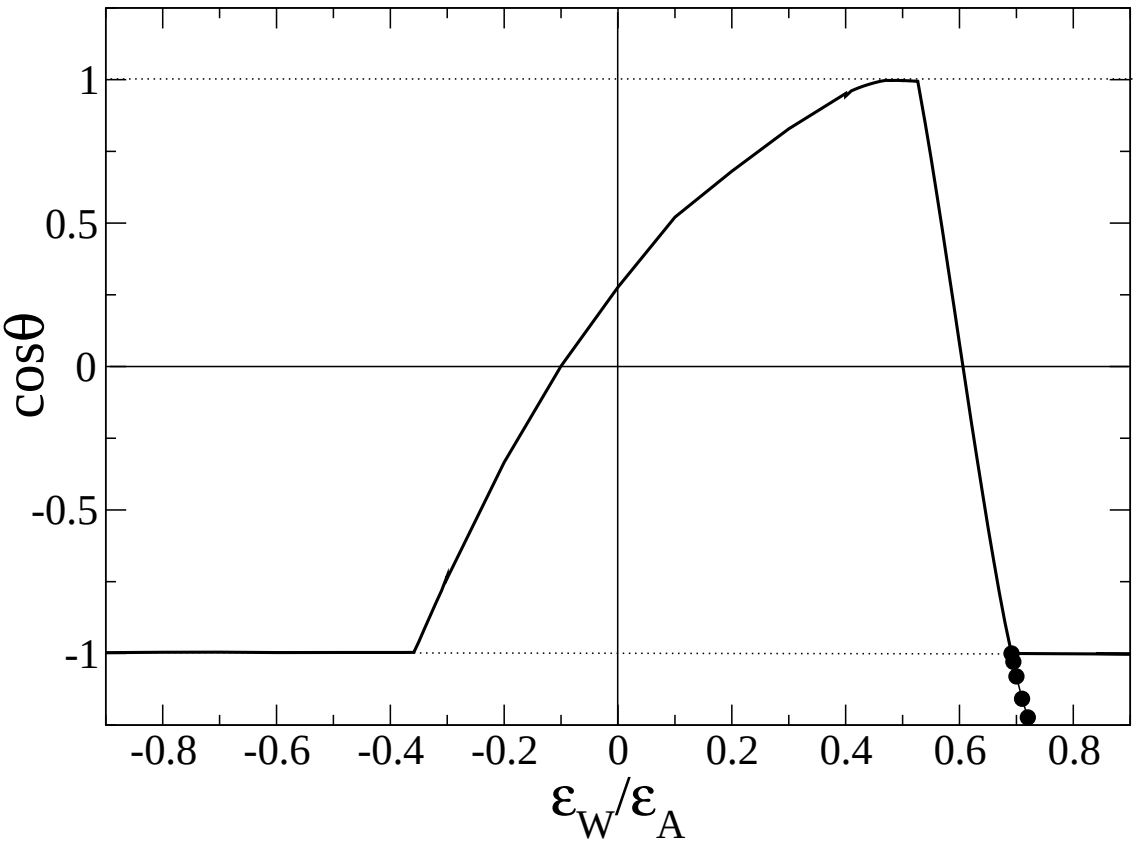

I. RODRIGUEZ-PONCE *et al*, FIGURE 3

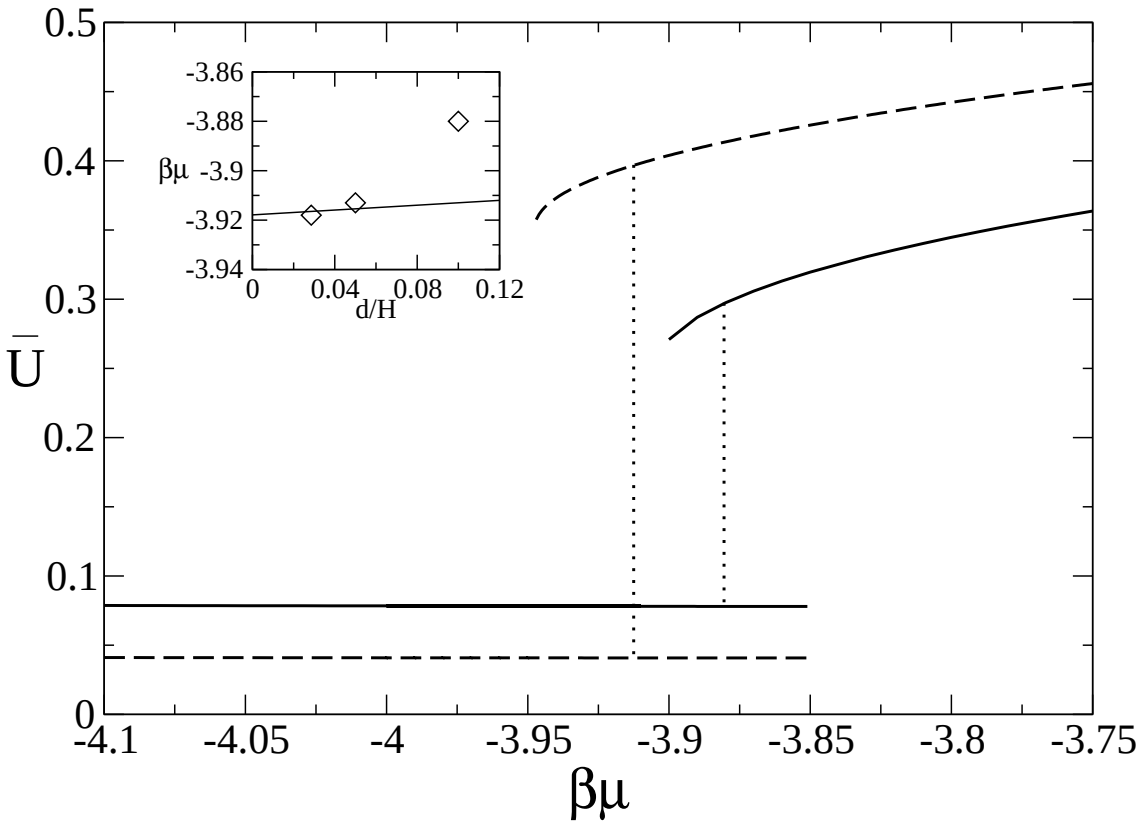

I. RODRIGUEZ-PONCE *et al*, FIGURE 4

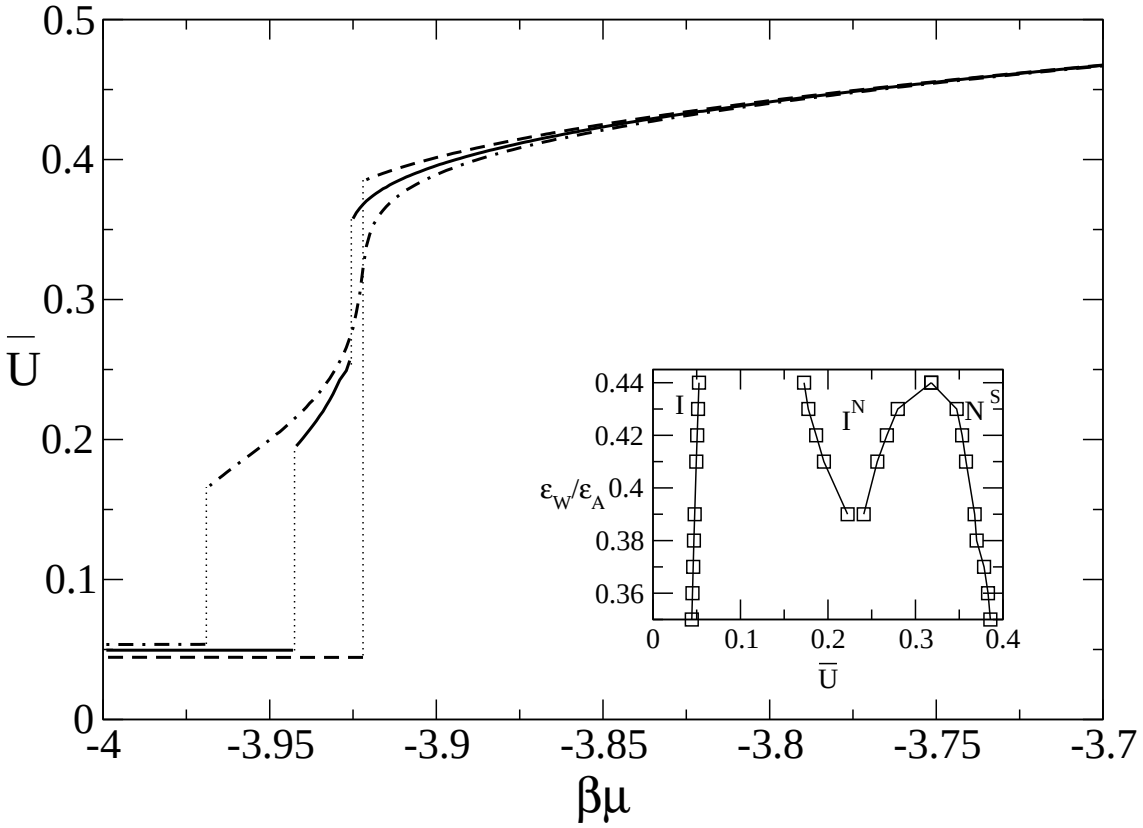

I. RODRIGUEZ-PONCE *et al*, FIGURE 5

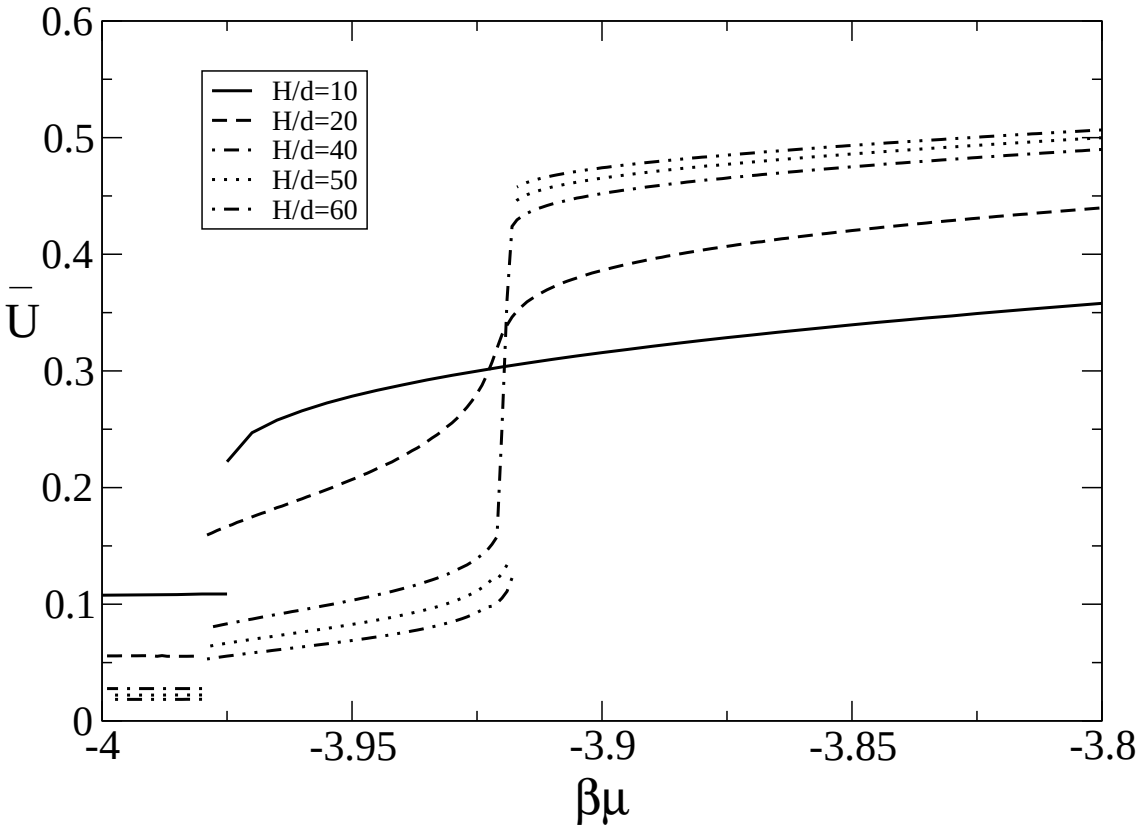

I. RODRIGUEZ-PONCE *et al*, FIGURE 6

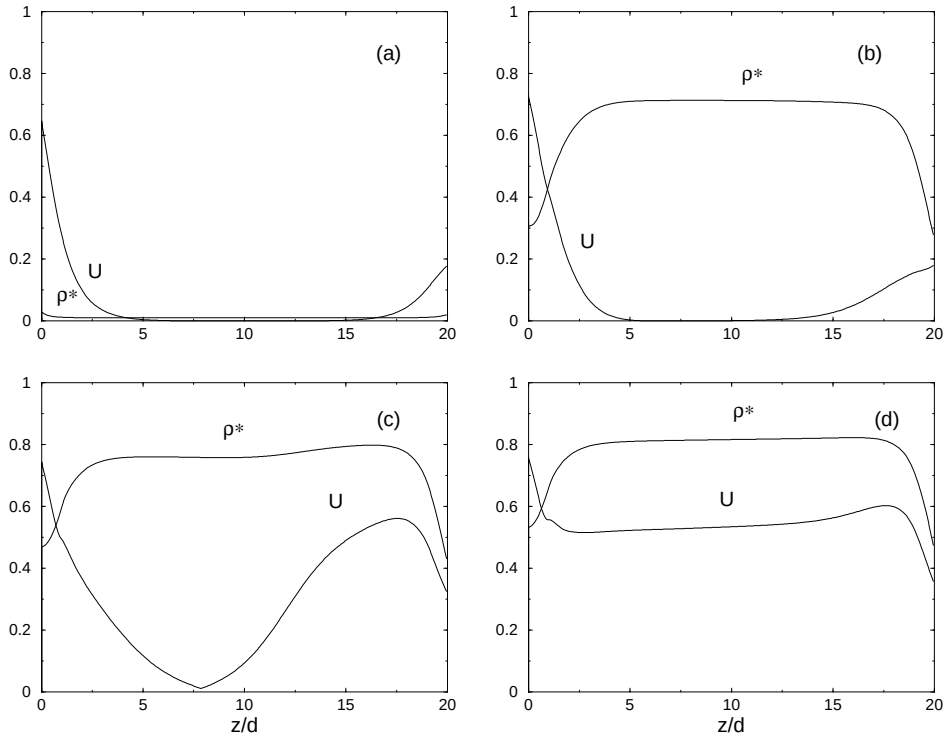

I. RODRIGUEZ-PONCE *et al*, FIGURE 7

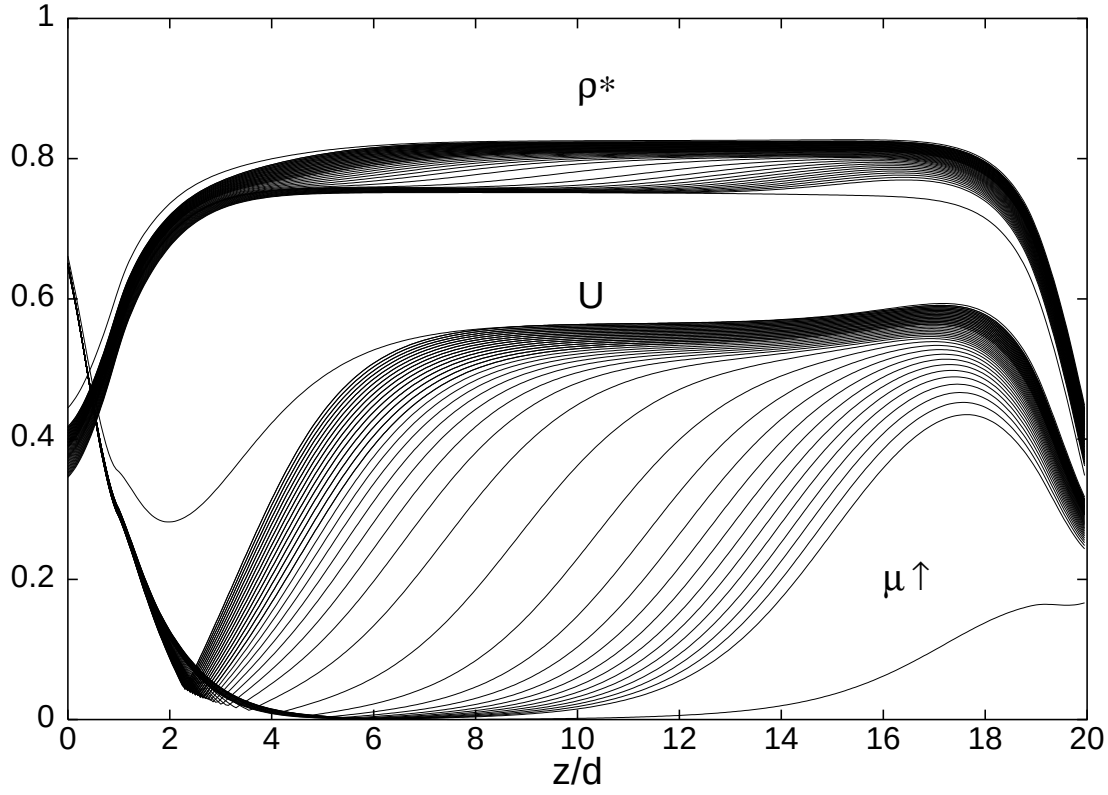

I. RODRIGUEZ-PONCE *et al*, FIGURE 8

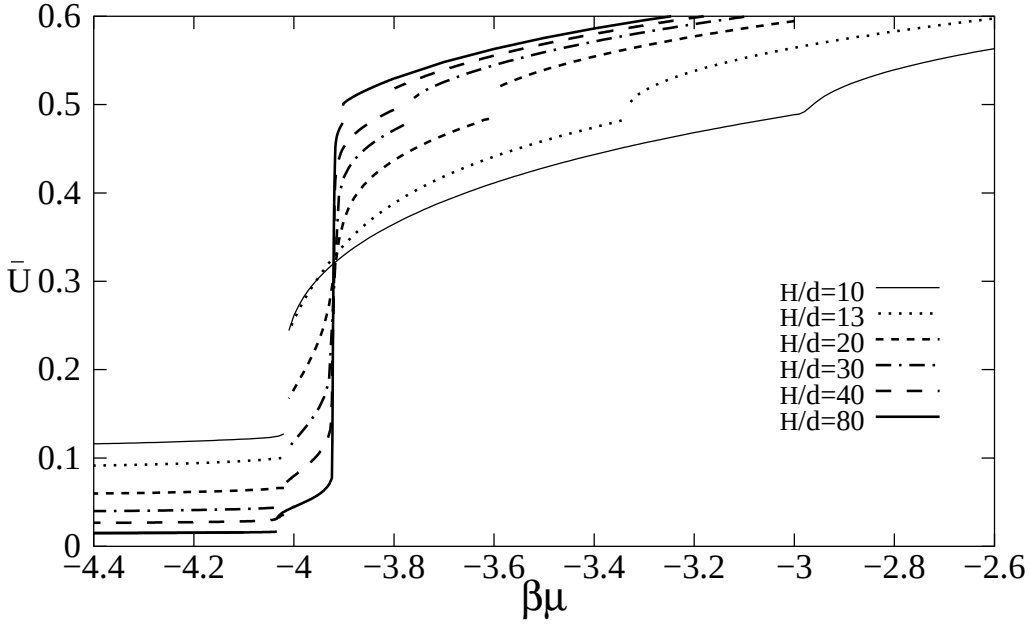

I. RODRIGUEZ-PONCE *et al*, FIGURE 9

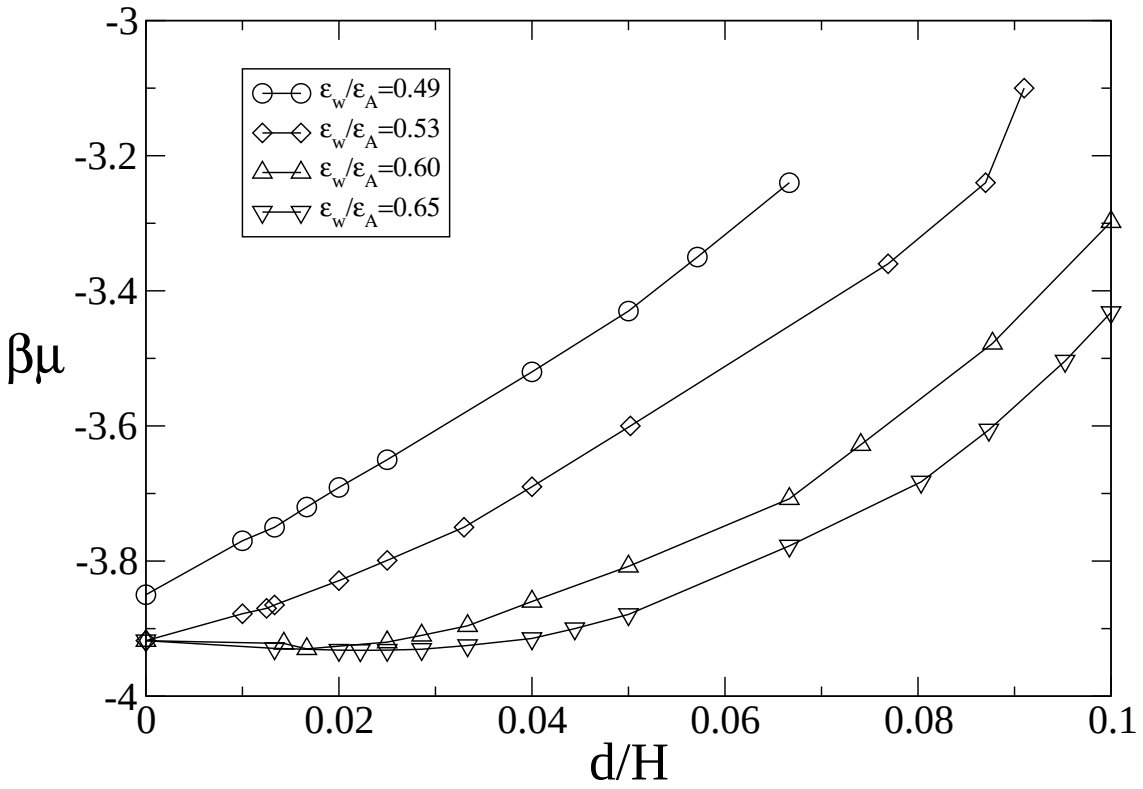

I. RODRIGUEZ-PONCE *et al*, FIGURE 10